PROCEEDINGS OF SCIENCE

Phenomenological description of young massive star clusters

Fabien Krayzel, Gilles Maurin, Giovanni Lamanna*
LAPP, Université Savoie Mont Blanc, CNRS/IN2P3, 9 Chemin de Bellevue, 74941 Annecy-le-Vieux, France
E-mail: Fabien.Krayzel@lapp.in2p3.fr, Gilles.Maurin.in2p3.fr, giovanni.lamanna@lapp.in2p3.fr

Alexandre Marcowith
LUPM, Université de Montpellier II, CNRS/IN2P3, Place Eugène Bataillon, 34095 Montpellier, France
E-mail: Alexandre.Marcowith@univ-montp2.fr

Nukri Komin
School of Physics, University of the Witwatersrand, 1 Jan Smuts Avenue, Braamfontein, Johannesburg, 2050 South Africa.
E-mail: nukri.komin@wits.ac.za

Most of the massive stars appear grouped in giant molecular clouds. Their strong wind activity generates large structures known as super bubbles and induces collective effects which could accelerate particles up to high energy and produce gamma-rays. The best objects to observe these effects are young massive star clusters in which no supernova explosion has occurred yet. Such star associations are typically still embedded in their parent molecular cloud, which can be traced traced out by the stellar light (HII region) emission due to ionization. Modelling this region such as a spherical. Considering this region as a spherical leaky-box surrounding a central cosmic ray source, a phenomenological model has been developed to estimate cosmic-rays and gamma-rays production for a set of selected clusters. In particular the expected high-energy gamma-ray emission has been finally estimated and compared to the present and future gamma-ray telescopes sensitivities.

The 34th International Cosmic Ray Conference,
30 July- 6 August, 2015
The Hague, The Netherlands

*Speaker.

PoS(ICRC2015)456

1. Introduction

Most of the massive stars are born, live and die for most of them in clusters. A rich and dense population of massive stars can be harboured in massive star clusters (MSC) hosting winds that can interact each other directly [1]. The mechanical energy imparted in the winds of the most massive stars over their lifetime can be equivalent to the mechanical energy deposited by a supernova. It is widely accepted that the remnants of supernovae are among the possible sites of cosmic particle acceleration [2], but it may also happen that the interaction of massive star winds in a cluster drives particle acceleration. In this work we test this hypothesis with respect to gamma-ray sensitivity of on-going facilities as well as the future performances of the Cherenkov Telescope Array (CTA). To that aim, we have developed a simple one-zone model where gamma-ray radiations are produced by cluster-accelerated particles interacting with the matter in dense surrounding HII regions. We have selected from different catalogues a list of MSCs young enough to not harbouring any supernova.

2. Modelling description

As in our previous work [3], we have made several assumptions in order to provide some simple predictions about the expected gamma-ray signal from young massive star clusters. We first assume that a fraction ξ of the stellar wind luminosity L_w released by the central cluster is converted into energetic particle power P_p :

- For protons : $P_p = \xi_p \, L_w$
- For electrons : $P_e = \xi_e L_w = K_{ep} \, \xi_p \, L_w$, where K_{ep} is the *e/p* ratio.

Where L_w is assumed to be constant as function of the time. Our model has basically two main regions: a region 1: the massive star cluster where particles are accelerated by collective shock acceleration, a region 2: the HII region engulfing the stellar cluster. For simplicity we assume spherical geometry in this work (see figure 1).

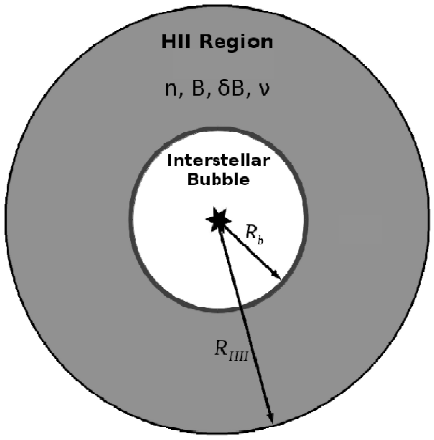

Figure 1: Geometrical shape of the model considering $R_b << R_{HII}$

The sizes of region 1 and 2 are considered constant as a function of the time and the size of the bubble is negligible compared to the one of the HII region. This implies that the HII region is the region of emission.

As detailed in [4], the following one-zone approximation is used to describe the particle spectrum in region 2:

$$\frac{\partial N}{\partial t} = \frac{\partial}{\partial E}(PN) - \frac{N}{\tau_{esc}} + Q \,, \tag{2.1}$$

where $Q \equiv Q(E,t)$ is the source term due to the acceleration process occurring in region 1, $\tau_{esc} \equiv \tau_{esc}(E)$ is the escape time : the characteristic time needed for energetic particles to escape from the HII region. In the following paragraphs we detail each parameter of equation 2.1 : injection, escape and losses of the energetic particles.

2.1 Injection from the bubble

The source term $Q(E,t)$ is linked with the energetic particle power by :

$$P_{RC} = \xi L_w = \int_V \int_{E_{inj}}^{E_{max}} Q(E,t) E \, dE \, d^3r \sim V_b \int_{E_{inj}}^{E_{max}} Q_0 \left(\frac{E}{E_{inj}}\right)^{-s} E \, dE \tag{2.2}$$

where E_{inj} is the injection energy, E_{max} the maximum energy reached by the particle. It is not in our purpose in this simple approach to model the particle acceleration in this region. A power law injection $Q(E) \propto E^{-s}$ is assumed, where $s = 2$ is the index of injection. We also assumed a homogeneous particle distribution, hence the integral on the volume can be replaced by the volume of the bubble V_b.

2.2 Escape from the HII Region

In the case of an isotropic 3D diffusion process, the escape time can be written as :

$$\tau_{esc}(E) = \frac{R_{HII}(t)^2}{6\, D(E)} \tag{2.3}$$

where R_{HII} is the HII region radius and D(E) the spatial diffusion coefficient inside the HII region. The latter is supposed to be proportional to the local galactic diffusion coefficient D_0 whose the value at 3 GeV is $D_{0,3\mathrm{GeV}} \approx 4 \times 10^{28}$ cm^{-1}.s^{-1} (deduced from the B/C ratio). Consequently :

$$D(E) = \left(\frac{D}{D_0}\right) \times D_{0,3\mathrm{GeV}} \times \left(\frac{E}{3\ \mathrm{GeV}}\right)^{2-\nu} \tag{2.4}$$

The coefficient is fixed by two parameters : the ratio D/D_0 and the index of turbulence ν. We have adopted a turbulence index $\nu = 5/3$ in the case of a Kolmogorov turbulence or $\nu = 3/2$ for the Iroshnikov-Kraichnan turbulence. The ratio D/D_0 is estimated from [5]. We end up with:

$$\begin{cases} \frac{D}{D_0} = \frac{1.2\times10^{-3}}{\eta} \times \left(\frac{\ell_{c,pc}}{B_{10}}\right)^{1/2} & \text{if } \nu = 3/2 \\ \frac{D}{D_0} = \frac{1.2\times10^{-2}}{\eta} \times \ell_{c,pc}^{2/3}\, B_{10}^{-1/3} & \text{if } \nu = 5/3 \end{cases} \tag{2.5}$$

Here we use the following notations: $\eta = \delta B^2/(\delta B^2 + B_0^2)$ is the turbulence level, δB is the intensity of the magnetic turbulence level and B_0 the mean intensity of the magnetic field, l_c the coherence length of the turbulent magnetic field, here fixed at 1 pc. Hereafter, two cases will be studied : $\delta B = 0.1 B_0$ for low magnetic turbulence level and $\delta B = B_0$ for a completely turbulent field. Finally, $B_{10} = B_0/10\mu$G.

2.3 Cooling in the HII Region

As the particles enter in the HII region, they suffer energy losses through several processes. For protons, the dominant loss process is pion production. Adiabatic losses do not play a role as the HII region has an approximate stationary size, the Coulomb interaction and ionization losses are negligible at the energies under consideration. For electrons, the following loss processes were considered :

- Inverse-Compton losses using various photon fields : Cosmic Microwave Background, Galactic photon field and the light from the cluster itself is added. The latter is just a sum of black-bodies from each O stars of the stellar cluster : its content in O stars is know thanks to the GOSC catalogue (see the section 4 for the details of the cluster selection from this catalogue).
- Synchrotron losses which depend on the magnetic field in the HII region.
- Bremsstrahlung losses which depend on the density of the HII region.

2.4 Solution of the one-zone model

The energetic particle spectrum in the HII region is given by the following analytical solution of the one-zone equation 2.1:

$$N(E,t) = \frac{1}{P(E)} \int_0^t P(E_t)\, Q(E_t,t')\, \exp\left(- \int_{t'}^t \frac{\mathrm{d}x}{\tau_{esc}(E_x)}\, \mathrm{d}t' \right) \tag{2.6}$$

where E_t is the energy of a particle at an instant $t' < t$ with an energy E at a instant t given by :

$$t - t' = \int_{E_e}^{E_t} \frac{\mathrm{d}E'}{P(E')} \tag{2.7}$$

This solution is valid as the energy losses are independent of time and the particle injection is quasi-stationary. Besides a stationary particle injection is assumed.

2.5 Summary of the modelling procedure

The model depends on several parameters generally fixed or constrained by observations :

- The HII region radius R_{HII} and density n_{HII} fixed by optical observations.
- The age and the distance from the earth are fixed by optical and/or IR observations.
- The stellar wind luminosity L_w is obtained from the cluster stellar content.
- The size of the interstellar bubble is deduced from optical observations.

Our free parameters are (even if they have some limitations):

- The conversion efficiency $\xi < 1$
- The *e/p* ratio K_{ep} for which the range $[10^{-4}, 10^{-2}]$ can be reasonably used.
- The magnetic field in the HII region which is at least equal the mean Galactic field, 3 μG and which could hardly be higher than 100 μG [6].
- The magnetic field turbulence level $0.1 < \delta B < 1$.
- The index of turbulence $\nu = 5/3$ or $3/2$.
- The index of injection which is conservatively fixed at $s = 2$.

3. Results

In order to understand the overall behaviour of young clusters, we define a typical cluster of 1 My with a HII region radius R_{HII} fixed to 10 pc and a density between 10 and 1000 cm^{-3}.

3.1 Characteristic times and stationarity

Figure 2 compares the characteristic times of losses (inverse Compton with CMB and star light, synchrotron, bremsstrahlung, pion decay) to the escape time according to the density, the index of turbulence and the magnetic field (intensity and turbulence level). A physical process is especially prominent if its characteristic time is short.

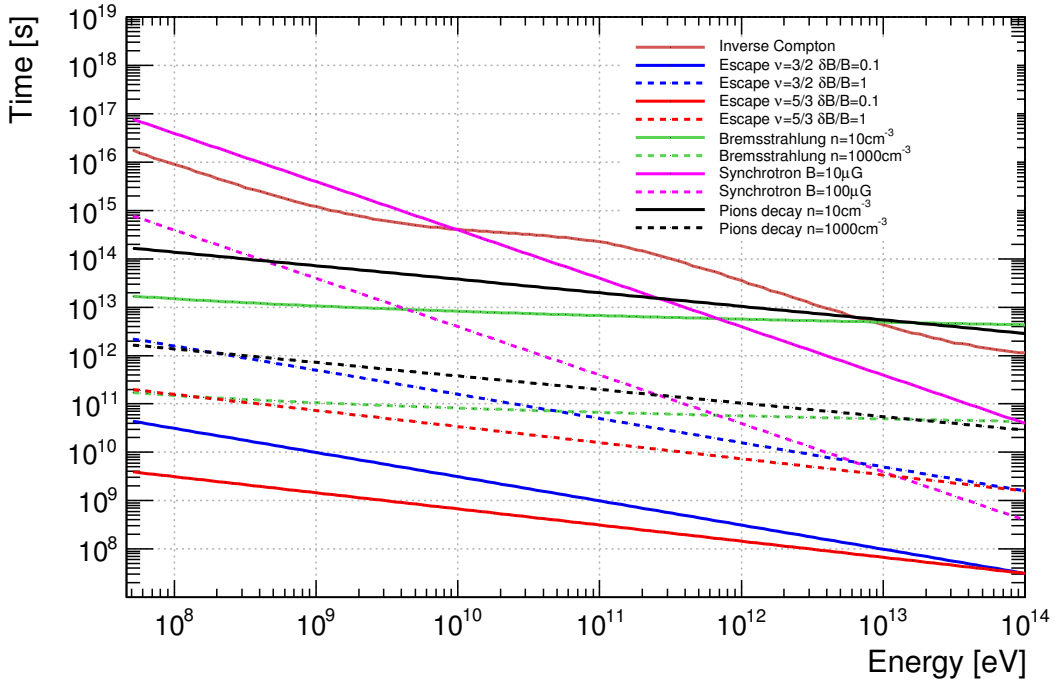

Figure 2: Characteristic times for loss processes and escape assuming a typical cluster of 1 My with a HII region radius R_{HII} fixed to 10 pc and a density between 10 and 1000 cm^{-3}.

For low density, all processes are largely dominated by escape losses to the exception of the synchrotron emission with a high magnetic field, but such magnetic field is expected only at high densities. At high densities and low turbulence level, the escape still dominates the other processes. But at a high turbulence level, synchrotron losses can be dominant at very high energy if the magnetic field is strong. Bremsstrahlung losses becomes dominant at lower energies.

These results call for some remarks. First, escapes dominate the other processes in most of the cases. This validates the assumption of a leaky-box model. Second, as one process dominates it results in monotonous spectra, especially in the case of proton emission. Finally, the characteristic times of the dominant processes are well below the cluster age at high energy. Steady state is then easily achieved, notably at high densities. Other more complete studies, not presented in this article, confirms this result.

3.2 Typical particle distributions

The left figure 3.2 shows the proton spectra obtained for a typical cluster and a powerlaw injection with an index $s = 2$. At low densities, proton spectrum is slightly sensitive to the index of turbulence and to the magnetic field turbulence level. It follows a powerlaw distribution with an index close to -2.25. For high densities, increasing turbulence level raises the proton spectrum at low energy. The spectrum softens and then reaches an index of -2.4.

The right figure 3.2 presents the electron spectra. At low energy, the spectrum softens at high densities because of Bremsstrahlung losses. At high energy, the spectrum drops due to synchrotron losses.

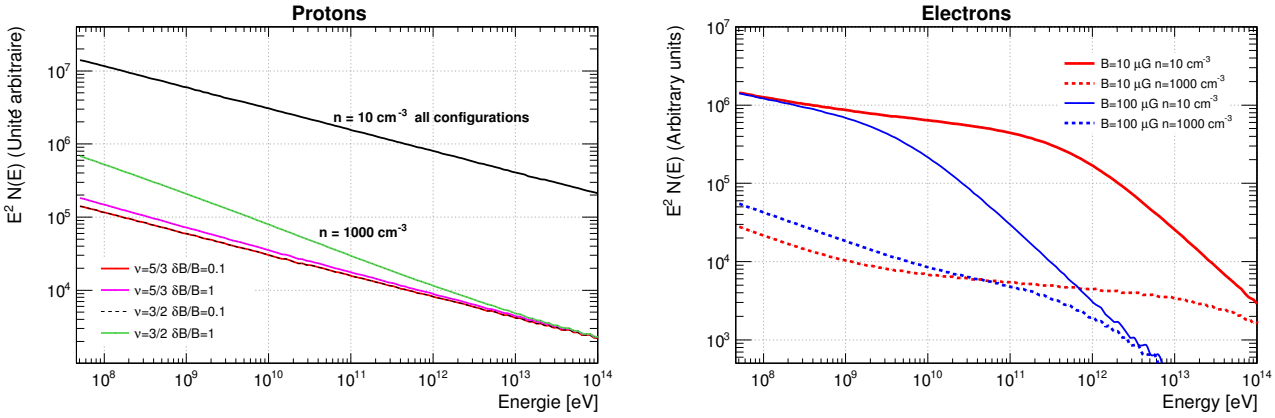

Figure 3: Proton and electron spectra for a typical cluster of 1My with a HII region radius R_{HII} fixed to 10 pc and a density between 10 and 1000 cm^{-3}.

4. Prediction for non-thermal emission

Our simple one-zone model can predict non-thermal emission at high energy. The main result is that non-thermal emissions are clearly dominated by the pion decay due to the high density in these objects. This result is robust considering parameters in realistic boundaries.

Thanks to the GOSC catalogue [7] listing O-stars, we select 10 clusters corresponding to our model (age, no SNR, no WR, close to a spherical shape...) and for which we know astrophysical

properties. Table 1 presents the estimated fluxes at 1 GeV and at 1 TeV assuming realistic parameters : B=10 μG, $K_{ep} = 10^{-2}$, $\xi = 10^{-2}$ and $\nu = 3/2$

Name	R_{HII} (pc)	n_{HII} (cm^{-3})	Log(Age) (ans)	D (kpc)	$\delta B/B = 0.1$		$\delta B/B = 1$	
					$\phi_{1\,GeV}$ (10^{-13} erg.cm^{-2}.s^{-1})	$\phi_{1\,TeV}$	$\phi_{1\,GeV}$ (10^{-13} erg.cm^{-2}.s^{-1})	$\phi_{1\,TeV}$
NGC 6193	39.7	11	6.0	1.3	8700	4600	11000	4700
NGC 2175	24	13	6.3	2.2	150	67	160	67
NGC 2244	16.9	15	6.28	1.55	20	9.5	25	9.7
NGC 3324	6.5	33	6.4	3	9.2	5.5	9.4	5.5
RCW 8	4.4	91	6.78	4.2	0.04	0.026	0.041	0.026
RCW 62	51.2	430	6.8	2.2	590	310	2800	910
NGC 6618	8	470	6	1.6	38	28	61	28
NGC 2467	8	550	6.3	4.1	2.6	1.9	4.6	1.9
NGC 6523	10	1600	6.2	1.8	250	160	1300	320
NGC 1976	3.7	8900	6.4	0.4	14	11	64	16

Table 1: For each cluster, table 1 summarises the important astrophysical parameters of the model : the HII region radius R_{HII}, the density n_{HII} are fixed by optical observations, its age and distance. Then this table gives the estimated fluxes at 1 GeV and at 1 TeV assuming B=10 μG, $K_{ep} = 10^{-2}$, $\xi = 10^{-2}$ and $\nu = 3/2$.

NGC 6193 seems to be a very promising cluster regardless of the magnetic turbulence level. Actually, this cluster contains the nearest O3-type star to earth. Unfortunately, the shape of its HII region is substantially away from a spherical shape, which may suggest that our model is less relevant.

Except for RCW 8, predicted fluxes for all other clusters, assuming a mechanical energy conversion of 1%, are accessible to Fermi-LAT [8] (differential sensibility between 10^{-12} and 10^{-11} erg.cm^{-2}.s^{-1} at 1 GeV). In a separate contribution [9], we use precisely Fermi-LAT observations and this model to constrain the conversion efficiency ξ for two clusters : NGC 2244 (the Rosette nebula) and NGC 1976 (the Orion nebula).

These clusters will also be reachable by the next generation of imaging atmospheric Cherenkov telescopes. Indeed CTA array should reach a sensitivity around 10^{-13} erg.cm^{-2}.s^{-1} at 1 TeV in 50 hours [10].

5. Conclusion

This article presents a simple one-zone model for young massive star clusters. It assumes that all stars are at the center of a spherical HII region. The latter is then treated as a leaky-box which allows to extract electron and proton spectra and then to deduce the expected non-thermal emissions. Considering realistic parameters steady state is quickly achieved compared to the cluster age and non-thermal emissions are clearly dominated by the pion decay due to the high density in the HII region.

Using this model, fluxes from 10 clusters are predicted. Assuming 1% conversion of the stellar wind energy, Fermi-LAT and CTA should be able to study the majority of these clusters.

In the absence of any signal at GeV or TeV energy regimes and after a long exposure, important constraints will although be deduced on the phenomenological model described in this work.

References

[1] E. Parizot, A. Marcowith, E. van der Swaluw, A. Bykov, and V. Tatischeff, *Superbubbles and energetic particles in the galaxy. 1. Collective effects of particle acceleration*, *Astron.Astrophys.* **424** (2004) 747–760, [astro-ph/0405531].

[2] L. O. Drury, J. Meyer, and D. Ellison, *Interpreting the cosmic ray composition*, astro-ph/9905008.

[3] F. Krayzel, A. Marcowith, G. Maurin, N. Komin, and G. Lamanna, *Young star clusters as gamma ray emitters and their detection with Cherenkov Telescopes*, in *ICRC*, 2013. no 0905.

[4] F. Aharonian and A. Atoyan, *Broad-band diffuse gamma-ray emission of the galactic disk*, *Astron.Astrophys.* **362** (2000) 937, [astro-ph/0009009].

[5] A. Marcowith and F. Casse, *Postshock turbulence and diffusive shock acceleration in young supernova remnants*, *Astron.Astrophys.* **515** (2010) A90, [arXiv:1001.2111].

[6] L. Harvey-Smith, G. J. Madsen, and B. M. Gaensler, *Magnetic Fields in Large Diameter HII Regions Revealed by the Faraday Rotation of Compact Extragalactic Radio Sources*, *Astrophys.J.* **736** (2011) 83, [arXiv:1106.0931].

[7] J. M. Apellaini, *The galactic o-star spectroscopic survey*, *Highlights of Spanish Astro- physics VI* (2011).

[8] W. B. Atwood, A. A. Abdo, M. Ackermann, W. Althouse, B. Anderson, M. Axelsson, L. Baldini, J. Ballet, D. L. Band, G. Barbiellini, and et al., *The Large Area Telescope on the Fermi Gamma-Ray Space Telescope Mission*, *ApJ* **697** (June, 2009) 1071–1102.

[9] F. Krayzel, N. Komin, G. Maurin, A. Marcowith, and G. Lamanna, *Constrains on particle acceleration in rosette and orion nebulae with fermi-lat observations*, in *ICRC*, 2017. no. 76.

[10] K. Bernlöhr, A. Barnacka, Y. Becherini, O. Blanch Bigas, E. Carmona, P. Colin, G. Decerprit, F. Di Pierro, F. Dubois, C. Farnier, S. Funk, G. Hermann, J. A. Hinton, T. B. Humensky, B. Khélifi, T. Kihm, N. Komin, J.-P. Lenain, G. Maier, D. Mazin, M. C. Medina, A. Moralejo, S. J. Nolan, S. Ohm, E. de Oña Wilhelmi, R. D. Parsons, M. Paz Arribas, G. Pedaletti, S. Pita, H. Prokoph, C. B. Rulten, U. Schwanke, M. Shayduk, V. Stamatescu, P. Vallania, S. Vorobiov, R. Wischnewski, T. Yoshikoshi, A. Zech, and CTA Consortium, *Monte Carlo design studies for the Cherenkov Telescope Array*, *Astroparticle Physics* **43** (Mar., 2013) 171–188, [arXiv:1210.3503].